Downlink Capacity of Super Wi-Fi Coexisting with Conventional Wi-Fi

Hyoil Kim, Kyubo Shin, and Changhee Joo
School of Electrical and Computer Engineering
Ulsan National Institute of Science and Technology (UNIST)
Ulsan, South Korea
Email: {hkim,kyubo,cjoo}@unist.ac.kr

***Abstract*—Super Wi-Fi is a Wi-Fi like service over TV white spaces (TVWS) based on the dynamic spectrum access (DSA) technology. Although Super Wi-Fi is expected to achieve larger coverage than conventional Wi-Fi thanks to the superior propagation characteristics of TVWS, it suffers from smaller bandwidth than Wi-Fi (6–8 MHz versus 20 MHz) which degrades network capacity. Therefore, it is common belief that the two Wi-Fi technologies may target different applications such as Super Wi-Fi for coverage and Wi-Fi for speed. However, there is a lack of studies that rigorously analyzes and compares the performance of Super Wi-Fi and Wi-Fi to confirm such belief. To fill the gap, this paper performs a thorough analysis on the capacity of Super Wi-Fi under the scenario that a Super Wi-Fi access point (AP) coexists with a Wi-Fi AP. Comparing the downlink capacity of Super Wi-Fi and Wi-Fi reveals that Super Wi-Fi can outperform Wi-Fi at the outskirts of the Wi-Fi's coverage and Super Wi-Fi gets more beneficial when channel bonding is employed. In addition, the maximal coverage radius of Super Wi-Fi is derived with which Super Wi-Fi can achieve better average capacity than a network of densely-deployed Wi-Fi APs, where the maximal radius is up to 3.2 times larger than the coverage radius of Wi-Fi.**

I. Introduction

Dynamic spectrum access (DSA) is a new way of utilizing spectrum resources that allows unlicensed users to opportunistically utilize spectrum *white spaces* (WS) in the licensed bands. Adoption of DSA by the market has been facilitated by new ruling and regulations released by the FCC (Federal Communications Commission) [1], [2]. In 2008, the FCC allowed unlicensed radio operation in the DTV bands, where the maximum transmission power is set as 4 W for fixed devices and 100 mW for personal/portable devices [1]. In 2010, the FCC finalized the rules that make the unused spectrum in the TV bands available for unlicensed broadband wireless devices, and resolved legal and technical issues in deploying such devices [2].

DSA is expected to introduce new applications in commercial, public, and military networks. For example, IEEE 802.22 WRAN (Wireless Regional Area Network) [3] is the first international DSA standard that aims to provide broadband Internet access for the fixed devices in the rural area, while Ecma 392 [4] is the first cognitive radio (CR) networking standard for personal/portable devices. In addition, IEEE 802.11af [5] is an IEEE 802.11 amendment for WLAN operation in TV white spaces (TVWS). The DSA technology can also be used in smart grid networks such as in the AMI (Advanced Metering Infrastructure) to carry information between smart meters and a network gateway [5].

Among them, IEEE 802.11af is one realization of the 'Super Wi-Fi' vision that tries to realize Wi-Fi-like Internet access using spectrum WS [6], [7]. Super Wi-Fi is expected to resolve the limitations of conventional Wi-Fi (henceforth simply referred to as Wi-Fi) such as small coverage and shaded areas, thanks to the superior propagation characteristics of the TVWS such as reduced path-loss and the wall-penetrating ability [8]. Super Wi-Fi, however, suffers from the smaller bandwidth in TV bands (6–8 MHz) than Wi-Fi (20 MHz) which limits the achievable network capacity. Hence, it is common belief that the two technologies target different applications, e.g., Super Wi-Fi for coverage and Wi-Fi for speed.

Nevertheless, there is a lack of studies that rigorously analyzes and compares the performance of Super Wi-Fi and Wi-Fi. Therefore, this paper performs a thorough analysis on the capacity of Super Wi-Fi to show whether it has potential to perform better than Wi-Fi. In particular, we investigate a scenario where a Super Wi-Fi AP coexists with a Wi-Fi AP, and consider the downlink capacity achieved by a mobile station that is capable of selectively utilizing either Super Wi-Fi or Wi-Fi. The results obtained from the analysis will play a crucial role to the successful adoption of Super Wi-Fi in the market in a way that they would be used to determine the strategic positions where Super Wi-Fi access points (APs) must be located so that their benefits can be maximized.

The main contribution of this paper is three-fold. First, we compare the downlink capacity of Super Wi-Fi and Wi-Fi to determine at which locations within the Wi-Fi's coverage Super Wi-Fi can be preferred to Wi-Fi. Second, we investigate the effect of channel bonding in further enhancing the performance of Super Wi-Fi. Finally, we derive the maximum radius of Super Wi-Fi's coverage to achieve better average capacity than a network of densely-deployed Wi-Fi APs.

The rest of the paper is organized as follows. Section II reviews the related work, and Section III investigates the downlink capacity of a Super Wi-Fi AP coexisting with a Wi-Fi AP and the impact of channel bonding. Section IV derives the maximum radius of Super Wi-Fi's coverage to achieve larger average capacity than a sea of Wi-Fi APs, and the paper concludes with Section V.

II. Related Work

Research on Super Wi-Fi is still in its infancy, and thus there exist only a limited number of publications in the literature. Among those, Simic et al. [9] provided a quantitative analysis of the performance of a network of Wi-Fi-like APs to obtain the downlink rate of the system. They considered the effects of inter-WS-AP interference, and confirmed that TVWS truly has favorable properties in achieving larger coverage. Kang et al. [10] considered coexistence between IEEE 802.22 and IEEE 802.11af over TVWS, and derived upstream and downstream performance of the 802.22 system. Hessar and Roy [11] studied the capacity of WS networks coexisting with a primary network of TV transceivers. Although [9]–[11] are somewhat related to ours, they did not consider Wi-Fi and Super Wi-Fi coexistence like ours. On the other hand, McGuire et al. [12] introduced rural broadband service in Scotland utilizing both 5 GHz UNII bands and TVWS that strikes a balance between throughput and coverage. Although they considered coexistence of Wi-Fi and WS devices that complement each other, no performance comparison has been provided between the two types of service.

In summary, our work has novelty in considering coexistence between Super Wi-Fi and Wi-Fi, and in providing analyses to determine the conditions where Super Wi-Fi is preferred to Wi-Fi.

III. Downlink Capacity of Super Wi-Fi Coexisting with Wi-Fi

In this section, we investigate the problem of Super Wi-Fi and Wi-Fi coexistence to determine the locations inside Wi-Fi's coverage where Super Wi-Fi achieves better downlink capacity than Wi-Fi. The analysis on this issue will provide the answer to our main motivation: whether Super Wi-Fi could also be beneficial to capacity, not only to coverage, from the perspective of a mobile station.

We first describe the network model for Super Wi-Fi and Wi-Fi coexistence. Suppose that in an x-y plane, a Wi-Fi AP (denoted by AP$_w$) is located at $(0, 0)$ and a Super Wi-Fi AP (denoted by AP$_s$) is located at $(d, 0)$ so that the two APs are apart by a distance of d meters, as shown in Fig 1. Without loss of generality, it is assumed that AP$_s$ is on the right-hand side of AP$_w$, i.e., $d \geq 0$. In the figure, R_w represents the coverage radius of Wi-Fi which will be discussed later in this section. Although the model considers only two APs, this setup is simple enough to provide us with key insights of the downlink capacity problem by focusing on a single user's point of view. Later in Section IV the scope will be extended to hexagonally-deployed APs to address the network provider's perspective.

Our model assumes an outdoor non-line-of-sight (NLOS) environment in a suburban area. It is expected that Super Wi-Fi and Wi-Fi coexistence will be encountered more often in suburban areas because (i) urban areas already have densely-deployed Wi-Fi networks, and (ii) rural areas are expected to be served by IEEE WRAN 802.22 [3]. Since the terrain profile of a suburban area includes two to five story buildings scattered throughout the region, an NLOS model is suitable

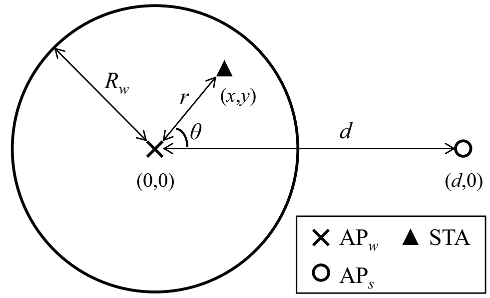

Fig. 1. Super Wi-Fi and Wi-Fi coexistence scenario.

for understanding the performance of Super Wi-Fi at various locations in the area.

Our objective is to find traces of (x, y) that satisfy $C_s \geq C_w$, where C_s and C_w represent downlink capacity of AP$_s$ and AP$_w$, respectively, each measured at (x, y). According to the Shannon's capacity theorem, the downlink capacities at (x, y) are expressed as

$$C_s = nB_s \log_2 \left(\frac{P_s d_s^{-\alpha_s}}{nN_s} + 1 \right), \tag{1}$$

$$C_w = B_w \log_2 \left(\frac{P_w d_w^{-\alpha_w}}{N_w} + 1 \right), \tag{2}$$

where d_s and d_w denotes the distance from (x, y) to AP$_s$ and AP$_w$, respectively, such as

$$d_s = \sqrt{(r \cos\theta - d)^2 + (r \sin\theta)^2}, \quad d_w = r. \tag{3}$$

In addition, B_s (or B_w), P_s (or P_w), α_s (or α_w), and N_s (or N_w) represent the bandwidth of a single channel, AP's transmit power, path loss exponent, and noise power within a single channel, respectively. The simplified path loss model has been adopted in Eqs. (1) and (2) since the objective of this work is to model the expected performance of Super Wi-Fi, not to predict terrain-specific signal propagation which may require empirical models like Okumura, Hata, and COST-231. The simplified model, however, can still capture the reality by utilizing empirically-predicted path-loss exponents.

In Eq. (1), n represents the number of TV channels to bond together by *Channel bonding*, which is a technique defined in IEEE 802.11af that merges multiple (possibly non-adjacent) channels into the one with larger bandwidth [13]. In 802.11af, there exist five channel bonding modes, TVHT_W, TVHT_W+W, TVHT_2W, TVHT_2W+2W, and TVHT_4W, that correspond to $n = 1$, $n = 2$, $n = 2$, $n = 4$, $n = 4$, respectively. In this paper, we consider $n = 1, 2$, where $n = 1$ is considered to study the baseline performance of Super Wi-Fi and $n = 2$ is considered to investigate the impact of channel bonding. Note that nN_s in Eq. (1) denotes the noise power in the bandwidth of nB_s since N_s is the noise power in a single channel.

The condition with which Super Wi-Fi is preferred to Wi-Fi is $C_s \geq C_w$, which leads to

$$nB_s \log_2\left(\frac{P_s d_s^{-\alpha_s}}{nN_s}+1\right) \geq B_w \log_2\left(\frac{P_w d_w^{-\alpha_w}}{N_w}+1\right). \quad (4)$$

Since outside the Wi-Fi coverage area Super Wi-Fi becomes the sole choice to (Super) Wi-Fi users, we focus on the case of $d_w \leq R_w$. The coverage radius of an IEEE 802.11 network is determined by the minimum receiver sensitivity defined in the standard, which is the minimum received signal strength at the receiver (in dBm) above which a signal is decodable. In this paper, we denote the minimum receiver sensitivity by RSS_{min}. Then, R_w is determined as

$$RSS_{min} = 10\log_{10}\frac{P_w {R_w}^{-\alpha_w}}{10^{-3}}, \quad (5)$$

$$\Rightarrow R_w = (10^{3-RSS_{min}/10}P_w)^{1/\alpha_w}. \quad (6)$$

By rearranging the terms in Eq. (4), we obtain

$$d_s \leq \rho_1\left(({d_w}^{-\alpha_w}+{\rho_2}^{-1})^{\rho_3}-{\rho_2}^{-\rho_3}\right)^{-1/\alpha_s}, \quad (7)$$

where $\rho_1, \rho_2, \rho_3 > 0$ are defined as

$$\rho_1 := \left(\frac{P_s/(nN_s)}{(P_w/N_w)^{B_w/(nB_s)}}\right)^{1/\alpha_s},$$

$$\rho_2 := \frac{P_w}{N_w}, \quad \rho_3 := \frac{B_w}{nB_s}. \quad (8)$$

By applying Eq. (3) to Eq. (7) and having both sides of the inequality squared, we derive

$$h(r,d) := \frac{r^2+d^2-{\rho_1}^2((r^{-\alpha_w}+{\rho_2}^{-1})^{\rho_3}-{\rho_2}^{-\rho_3})^{-2/\alpha_s}}{2rd} \leq \cos\theta. \quad (9)$$

Since $\cos\theta$ is monotonically decreasing with $\theta \in [0,\pi]$, we obtain Theorem 1.

Theorem 1. *In a scenario described in Fig. 1,*

1) *AP_s is always preferred by the station if*
   - $h(r,d) < -1$, *or*
   - $-1 \leq h(r,d) \leq 1$ *and* $0 \leq \theta \leq \cos^{-1}[h(r,d)]$.
2) *AP_w is always preferred by the station if*
   - $h(r,d) > 1$, *or*
   - $-1 \leq h(r,d) \leq 1$ *and* $\cos^{-1}[h(r,d)] < \theta \leq \pi$.

A. Illustrative Parameters used for Case Study

To get an intuition from Theorem 1, we consider the illustrative parameters in Table I. In the table, P_s is chosen as the maximum EIRP (effective isotropic radiated power) of portable WS devices [2],[1] and P_w is set as the typical transmission power of commercial Wi-Fi APs. In addition, N_s is chosen based on the noise PSD (power spectral density) of -163 dBm/Hz in TV bands [14] while $N_w = -90$ dBm is the reported noise level in outdoor WLANs at 2.4 GHz [15]. We set $RSS_{min} = -82$ dBm according to IEEE 802.11n.

[1]We assume omni-directional antennas with 0 dBi.

B_s	6 MHz	B_w	20 MHz
P_s	100 mW (20 dBm)	P_w	100 mW (20 dBm)
α_s	3.6	α_w	5.3
N_s	$10^{-12.52}$ W (-95.2 dBm)	N_w	10^{-12} W (-90 dBm)

TABLE I
ILLUSTRATIVE PARAMETERS OF SUPER WI-FI AND WI-FI

α_s and α_w are set according to [16] which performed field measurements at 900 MHz and 1,900 MHz in NLOS outdoor suburban environments using the same terrain profile.[2] The impact of multi-path fading on signal propagation is taken account with thus-determined exponents since the measurements are obtained under the influence of fading. In addition, the chosen values well capture the fact that path loss exponents tend to increase at higher frequencies [17].

B. A Special Case: $d = 0$ (i.e., AP$_s$ and AP$_w$ are co-located)

In the special case of $d = 0$, we have $d_s = d_w = r$, $0 < r \leq R_w$.[3] Then, Eq. (7) becomes

$$g(r) := r - \rho_1\left((r^{-\alpha_w}+{\rho_2}^{-1})^{\rho_3}-{\rho_2}^{-\rho_3}\right)^{-1/\alpha_s} \leq 0. \quad (10)$$

Numerically evaluating Eq. (10) using the parameters in Table I reveals that $g(r) > 0$ for $0 < r < r^\dagger$ and $g(r) < 0$ for $r^\dagger < r \leq R_w$, where

$$r^\dagger := = \begin{cases} 61.77, & n = 1, \\ 22.88, & n = 2. \end{cases} \quad (11)$$

That is, AP$_s$ is preferred to AP$_w$ for $r^\dagger < r \leq R_w$ while AP$_w$ is preferred to AP$_s$ for $0 < r < r^\dagger$.

The result in Eq. (11), however, is specific to the parameters chosen in Table I. From now on, we generalize the result to arbitrary parameters by deriving a sufficient condition regarding α_s/α_w under which a unique threshold $r^\dagger$ exists such that AP$_s$ is preferred to AP$_w$ for $r \in (r^\dagger, R_w]$ and vice versa for $r \in (0, r^\dagger)$.[4] We assume that $n = 1, 2$, and $\alpha_s < \alpha_w$.[5]

First, it is trivial to show $\lim_{r\to 0} g(r) = 0$, and $\lim_{r\to 0} g'(r) = 1$ for $n = 1, 2$. In case we additionally have $g''(r) < 0$ for $r \in (0, R_w]$ and $g(R_w) < 0$, there exists the unique distance threshold $r^\dagger \in (0, R_w)$. Hence, we will show that there exists $\delta \in (0, 1]$ such that $g''(r) < 0$ and $g(R_w) < 0$ for $\alpha_s/\alpha_w < \delta$ and $\alpha_s, \alpha_w \in [2, 6]$.[6] In particular, we try to determine the δ closest to 1 so that the derived δ may include as many conceivable pairs of (α_s, α_w) as possible.

[2]Although 900 MHz is slightly higher than TVWS (54–806 MHz) and 1,900 MHz is a bit lower than ISM bands (2.4 GHz), they are close enough to the bands of interest, and the work in [16] is among the few measuring the two separate bands in the same environment. Note that it is essential to utilize the path loss exponents that are measured under the same environment since path loss varies with the terrain profile.

[3]$R_w = 84.04$ meters if we apply the parameters in Table I to Eq. (6).

[4]We focus on the metric α_s/α_w because (α_s, α_w) varies significantly according to the terrain profile while other parameters do not.

[5]Note that $\alpha_s < \alpha_w$ always holds due to the superior signal propagation in TVWS.

[6]Note that path loss exponents are between 2 and 6 in most practical scenarios.

From Eq. (10), the condition $g(R_w) < 0$ corresponds to

$$\frac{\alpha_s}{\alpha_w} < \delta_1 := \frac{\ln\left(\frac{(10^{RSS_{min}/10-3}/P_w + {\rho_2}^{-1})^{\rho_3} - {\rho_2}^{-\rho_3}}{{\rho_1}^{\alpha_s}}\right)}{\ln\left(10^{RSS_{min}/10-3}/P_w\right)}, \quad (12)$$

where Eq. (6) is applied. Note that the right-hand side of Eq. (12) is independent of (α_s, α_w) since ${\rho_1}^{\alpha_s}$ does not depend on α_s by Eq. (8).

In addition, it can be shown that

$$g''(r) = \frac{(\rho_1\rho_3\alpha_w/\alpha_s)\cdot k(r)}{(1 + r^{\alpha_w}{\rho_2}^{-1})\{(1 + r^{\alpha_w}{\rho_2}^{-1})^{\rho_3} - (r^{\alpha_w}{\rho_2}^{-1})^{\rho_3}\}} \cdot \frac{r^{-\alpha_w-2}(r^{-\alpha_w} + {\rho_2}^{-1})^{\rho_3-1}}{\{(r^{-\alpha_w} + {\rho_2}^{-1})^{\rho_3} - {\rho_2}^{-\rho_3}\}^{1/\alpha_s+1}}, \quad (13)$$

$$k(r) := \left\{\left(1 - \alpha_w\rho_3/\alpha_s\right) + (1+\alpha_w)\frac{r^{\alpha_w}}{\rho_2}\right\}\left(1 + \frac{r^{\alpha_w}}{\rho_2}\right)^{\rho_3} - \left\{(1+\alpha_w\rho_3) + (1+\alpha_w)\frac{r^{\alpha_w}}{\rho_2}\right\}\left(\frac{r^{\alpha_w}}{\rho_2}\right)^{\rho_3} \quad (14)$$

Therefore, $g''(r) < 0$ is equivalent to $k(r) < 0$. By letting $x := r^{\alpha_w}/\rho_2$ and applying $\alpha_s/\alpha_w < \delta$, we obtain

$$\begin{aligned} k(x) < \psi(x) :=\ & \{\left(1 - \rho_3/\delta\right) + (1+\alpha_w)x\}(1+x)^{\rho_3} \\ & -\{(1+\alpha_w\rho_3) + (1+\alpha_w)x\}x^{\rho_3} \\ =\ & \{\left(1 - \rho_3/\delta + x\right)(1+x)^{\rho_3} - (1+x)x^{\rho_3}\} \\ & +\{x(1+x)^{\rho_3} - (\rho_3+x)x^{\rho_3}\}\alpha_w. \end{aligned} \quad (15)$$

Since $\psi(x)$ is linear with α_w, it is maximized at $\alpha_w = 2$ when $\{x(1+x)^{\rho_3} - (\rho_3+x)x^{\rho_3}\} < 0$ and at $\alpha_w = 6$ when $\{x(1+x)^{\rho_3} - (\rho_3+x)x^{\rho_3}\} > 0$. We want both maximum values upper-bounded by zero so that $\psi(x) \leq 0$. When maximized at $\alpha_w = 6$, it is sufficient to have $\left(1 - \rho_3/\delta + 7x\right) \leq 0$ which results in

$$\frac{\alpha_s}{\alpha_w} < \delta_2 := \frac{\rho_3}{1 + 7\cdot 10^{3-RSS_{min}/10}\cdot N_w}. \quad (16)$$

When maximized at $\alpha_w = 2$, it can be shown that $\psi(x) \leq 0$ is already satisfied by Eq. (16).

Therefore, we derive Theorem 2 as follows.

Theorem 2. *When a Super Wi-Fi AP and a Wi-Fi AP are co-located, for $n = 1, 2$, and $\alpha_s/\alpha_w < \min\{\delta_1, \delta_2, 1\}$,*
AP_s is preferred for $r^\dagger < r \leq R_w$, and
AP_w is preferred for $0 < r < r^\dagger$,
where $r^\dagger = \{r : g(r) = 0, 0 < r \leq R_w\}$, and δ_1, δ_2 are given as in Eqs. (12) and (16), respectively.

Note that α_w and α_s are likely to satisfy Eqs. (12) and (16) because they usually differ much due to the large frequency deviation between the two bands. For example, the chosen parameters in Table I satisfy Eqs. (12) and (16) since $\alpha_s/\alpha_w = 3.6/5.3 = 0.67$ and δ_1 and δ_2 are determined as

$$\delta_1 = \begin{cases} 0.84, & n = 1, \\ 0.96, & n = 2, \end{cases} \qquad \delta_2 = \begin{cases} 1.58, & n = 1, \\ 0.79, & n = 2. \end{cases} \quad (17)$$

Discussion: A public belief is that Super Wi-Fi is beneficial only for coverage since Wi-Fi is superior to Super Wi-Fi in terms of throughput. However, Theorem 2 indicates that a Super Wi-Fi AP may excel a co-located Wi-Fi AP in the outskirts of Wi-Fi's coverage. The distance threshold $r^\dagger$, beyond which Super Wi-Fi becomes preferred to Wi-Fi, decreases as n grows as shown in Eq. (11) and in Fig. 2.[7] Therefore, in the case of co-located APs, a Super Wi-Fi AP can be considered as a secondary service to Wi-Fi such that stations far away from the Wi-Fi AP can switch to Super Wi-Fi service to achieve better downlink capacity.

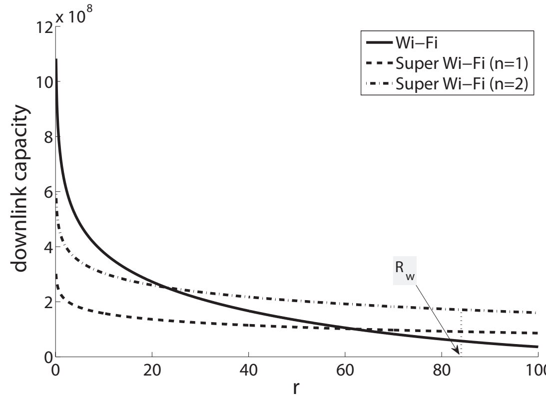

Fig. 2. Downlink capacity of co-located Super Wi-Fi and Wi-Fi.

C. Super Wi-Fi's Performance within Wi-Fi's Coverage

The aforementioned observations raises the following question: at which locations Super Wi-Fi will be preferred to Wi-Fi when the two APs are no longer co-located (i.e., $d \neq 0$)? To address this issue, we illustrate some representative cases in Fig. 3 while varying d as $0 \leq d \leq R_w$, where the shaded areas represent the locations at which Super Wi-Fi is preferred to Wi-Fi. The plots are drawn using Table I and Eq. (4).

Fig. 3 presents the scenario without channel bonding. When $d = 0$, Super Wi-Fi is preferred only in the outskirts area of AP_w's coverage as predicted in Sections III-B. As d grows, however, Super Wi-Fi becomes also preferred in the vicinity of AP_s. With channel bonding, as shown in Fig. 4, Super Wi-Fi becomes more preferred within Wi-Fi's coverage even in the inner region of Wi-Fi's coverage, except in the vicinity of AP_w. This verifies the significant benefit of channel bonding in extending Super Wi-Fi's preferred region.

Note that when a station is mobile, it compares the SNR of the two APs' signals and decide when to switch to the other AP according to the achievable capacity. The mechanism for this operation is beyond the scope of this paper.

IV. Maximal Coverage Radius of Super Wi-Fi to Outperform Wi-Fi

In Section III, a baseline study was performed considering a single Wi-Fi AP and a single Super Wi-Fi AP where we addressed a mobile station's perspective in determining which service it should utilize to maximize its downlink capacity. A Super Wi-Fi service provider, however, may have a different

[7] Fig. 2 is drawn by applying the parameters in Table I to Eqs. (1) and (2).

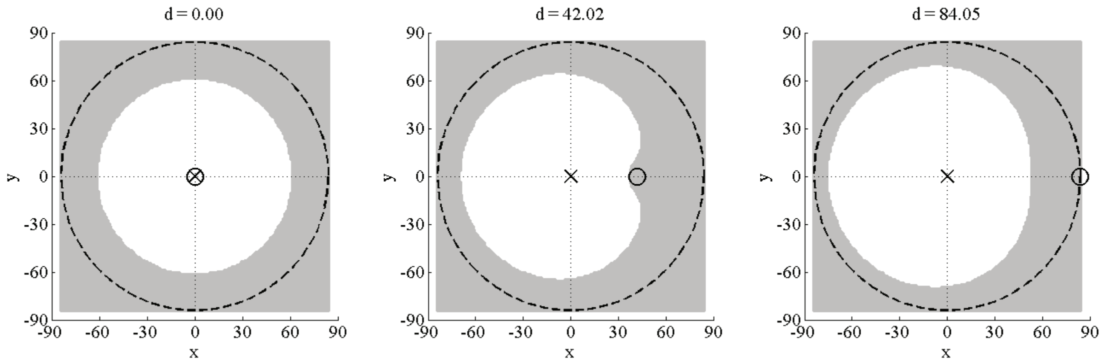

Fig. 3. Preferred region of Super Wi-Fi (the shaded area) within Wi-Fi's coverage: when $n = 1$ (no channel bonding).

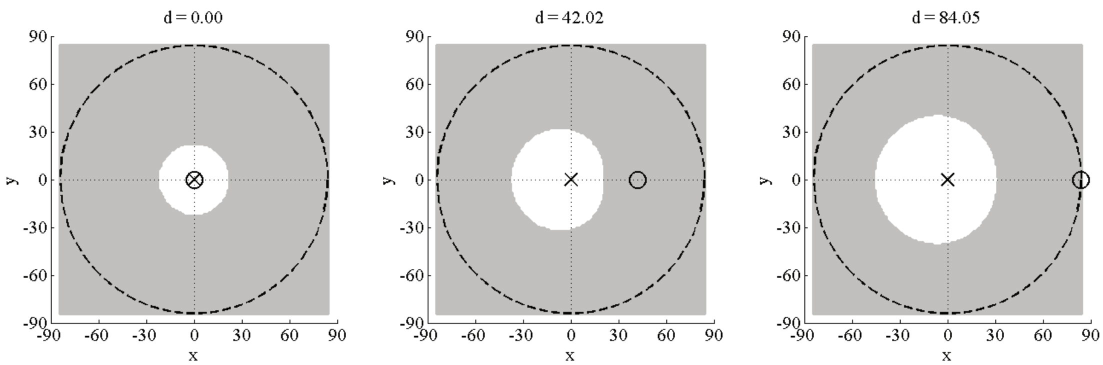

Fig. 4. Preferred region of Super Wi-Fi (the shaded area) within Wi-Fi's coverage: when $n = 2$ (channel bonding).

objective of strategically deploying Super Wi-Fi APs to maximize the average network capacity in its service area while achieving larger per-AP coverage than Wi-Fi. Therefore, in this section we focus on the network infrastructure provider's perspective.

In particular, we consider (i) a sea of hexagonally-deployed Wi-Fi APs each with the coverage radius of R_w, and (ii) a sea of hexagonally-deployed Super Wi-Fi APs each with the coverage radius of R_s, where the two networks coexist with each other. The hexagonal deployment is illustrated in Fig. 5 for Wi-Fi; the only difference in the case of Super Wi-Fi is the radius R_w in the figure is replaced with R_s. In such a scenario, we investigate the average downlink capacity of Wi-Fi and Super Wi-Fi, denoted by $\bar{C}_w$ and $\bar{C}_s$, respectively.

For any hexagonal cellular deployment, there exists a simple solution to three-coloring the graph where a vertex represents an AP, an edge represents a pair of adjacent APs, and a color represents a channel assigned to an AP. Thus-determined optimal channel assignment is shown in Fig. 5 using three channel indexes 1, 2, and 3 which confirms no AP would experience co-channel interference from its direct neighbor. Therefore, inter-AP interference can be effectively ignored in calculating per-AP average capacity, assuming centralized channel assignment by the network provider and no other same-type (i.e., Wi-Fi or Super Wi-Fi) contending providers. Note that assigning three non-overlapping channels is possible since 2.4 GHz Wi-Fi has three non-overlapping channels and

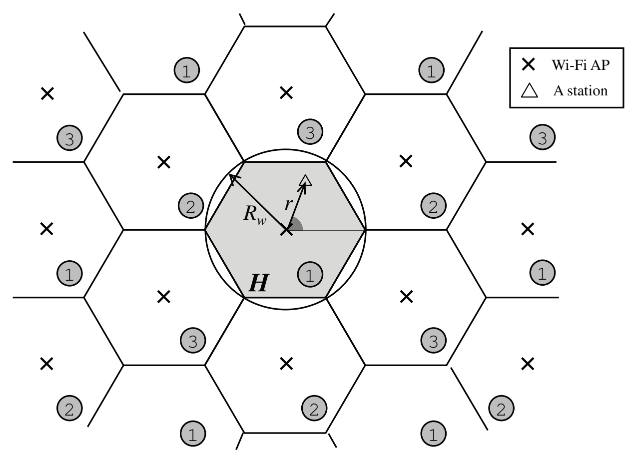

Fig. 5. Hexagonally-deployed Wi-Fi APs with radius R_w (Super Wi-Fi APs are similarly deployed with R_s).

TVWS-based Super Wi-Fi has 68 TV channels (from 2 to 69).

Regarding the average downlink capacity, we can focus on a certain AP's coverage H (the shaded region in Fig. 5) due to symmetry. In addition, we introduce a polar coordinate with (r, θ) as shown in Fig. 5, where r is modeled as a random variable R with probability density function (p.d.f.)

$$f_R(r) = \begin{cases} \frac{2r}{{r_{max}}^2}, & 0 < r < r_{max}, \\ 0, & \text{otherwise}, \end{cases}$$

where $r_{max} = R_s$ for Super Wi-Fi and $r_{max} = R_w$ for Wi-Fi, and θ is modeled as a random variable Θ uniformly distributed in $[0, 2\pi]$. The described model can represent mobile stations uniformly distributed in an AP's coverage area [18].

Then, $\bar{C}_s$ and $\bar{C}_w$ can be expressed as[8]

$$\bar{C}_s \simeq \int_0^{R_s} nB_s \log_2 \left(\frac{P_s r^{-\alpha_s}}{nN_s} + 1 \right) f_R(r) dr, \quad (18)$$

$$\bar{C}_w \simeq \int_0^{R_w} B_w \log_2 \left(\frac{P_w r^{-\alpha_w}}{N_w} + 1 \right) f_R(r) dr. \quad (19)$$

By assuming $P_s r^{-\alpha_s}/nN_s \gg 1$ and $P_w r^{-\alpha_w}/N_w \gg 1$, we can further approximate Eqs. (18) and (19) as

$$\begin{aligned}\bar{C}_s &\simeq \int_0^{R_s} nB_s \log_2 \left(\frac{P_s r^{-\alpha_s}}{nN_s} \right) \frac{2r}{R_s{}^2} dr \\ &= \frac{2nB_s}{R_s{}^2} \int_0^{R_s} \left\{ r \log_2 \frac{P_s}{nN_s} - \alpha_s \cdot r \log_2 r \right\} dr \\ &= nB_s \left\{ \left(\log_2 \frac{P_s}{nN_s} + \frac{\alpha_s}{2 \ln 2} \right) - \alpha_s \log_2 R_s \right\}, \quad (20)\end{aligned}$$

$$\bar{C}_w \simeq B_w \left\{ \left(\log_2 \frac{P_w}{N_w} + \frac{\alpha_w}{2 \ln 2} \right) - \alpha_w \log_2 R_w \right\}, \quad (21)$$

where the second assumption $P_w r^{-\alpha_w}/N_w \gg 1$ is derived by comparing $RSS_{min} = -82$ dBm and $N_w = -90$ dBm, and the first assumption is derived by considering the minimum sensitivity of IEEE 802.11af [19][9] and $N_s = -95.2$ dBm.

The form of Eq. (20) suggests that $\bar{C}_s$ gets smaller as R_s increases. Hence, we find the maximum R_s, denoted by R_s^{max}, below which we achieve $\bar{C}_s \geq \bar{C}_w$, i.e., the Super Wi-Fi network performs better than the Wi-Fi network on average. By comparing thus-measured $\bar{C}_w$ with Eq. (18) such that $\bar{C}_s \geq \bar{C}_w$, the maximum radius R_s^{max} is determined as

$$R_s^{max} = \begin{cases} 40.81, & n = 1, \\ 269.36, & n = 2, \end{cases}$$

from which it is seen that R_s^{max} without channel bonding (i.e., $n = 1$) achieves smaller coverage than $R_w = 84.04$ subject to $\bar{C}_s \geq \bar{C}_w$. Therefore, there is a tradeoff between coverage and capacity, i.e., if Super Wi-Fi wants to achieve larger coverage than Wi-Fi, it has to allow its average capacity to become inferior to Wi-Fi, and vice versa. R_s^{max} with channel bonding (i.e., $n = 2$), however, turns out to be 3.2 times larger than R_w, and thus we can conclude that Super Wi-Fi has potential to achieve larger coverage and larger capacity compared to Wi-Fi as long as channel bonding is supported.

V. Conclusion and Future Work

In this work, we have studied whether Super Wi-Fi can outperform Wi-Fi within Wi-Fi's coverage in terms of downlink capacity. By considering a Super Wi-Fi AP coexisting with a Wi-Fi AP, it is revealed that Super Wi-Fi can excel Wi-Fi in the outskirts of Wi-Fi's coverage, which becomes more prominent with channel bonding. The maximal coverage radius of a Super Wi-Fi network has been also derived so that a network of Super Wi-Fi APs may achieve better average capacity than a sea of Wi-Fi APs.

In future, we would like to consider the multi-station scenario where downlink capacity is shared between (Super) Wi-Fi users so that the impact of user population can be studied.

[8]Note that Eqs. (18) and (19) are approximations because the integration region is the circular area of an AP instead of the hexagonal area H.

[9]It is -88 dBm for $n = 1$ and -85 dBm for $n = 2$.

Acknowledgments

The work described in this paper was supported in part by the year of 2011 Research Fund of the UNIST (Ulsan National Institute of Science and Technology), and the Basic Science Research Program through the National Research Foundation of Korea (NRF) funded by the Ministry of Education, Science and Technology (2012R1A1A1014648).

References

[1] FCC, "Second Report and Order and Memorandum Opinion and Order," *ET Docket No. 08-260*, November 2008.
[2] FCC, "Second Memorandum Opinion and Order," *ET Docket No. 10-174*, September 2010.
[3] "IEEE 802.22 Working Group on Wireless Regional Area Networks." http://www.ieee802.org/22/.
[4] J. Wang, et al., "First Cognitive Radio Networking Standard for Personal/Portable Devices in TV White Spaces," in *IEEE DySPAN*, 2010.
[5] J. Wang, M. Ghosh, and K. Challapali, "Emerging Cognitive Radio Applications: A Survey," *IEEE Commun. Mag.*, pp. 74–81, March 2011.
[6] P. Bahl, R. Chandra, T. Moscibroda, R. Murty, and M. Welsh, "White Space Networking with Wi-Fi like Connectivity," in *Proc. ACM SIGCOMM*, 2009.
[7] H. Kim and K. Shin, "Understanding Wi-Fi 2.0: From The Economical Perspective of Wireless Service Providers," *IEEE Wirel. Commun.*, pp. 2–8, August 2010.
[8] J. Chapin and W. Lehr, "The Path to Market Success for Dynamic Spectrum Access Technology," *IEEE Commun. Mag.*, vol. 45, pp. 96–103, May 2007.
[9] L. Simic, M. Petrova, and P. Mahonen, "Wi-Fi, but not on Steroids: Performance Analysis of a Wi-Fi like Network Operating in TVWS under Realistic Conditions," in *Proc. IEEE ICC*, 2012.
[10] H. Kang, D. Lee, B.-J. Jeong, and A. Kim, "Coexistence between 802.22 and 802.11af over TV White Space," in *IEEE ICTC*, 2011.
[11] F. Hessar and S. Roy, "Capacity considerations for secondary networks in tv white space," *arXiv:1304.1785v1*, March 2013.
[12] C. McGuire, M. Brew, F. Darbari, S. Weiss, and R. Stewart, "Enabling Rural Broadband via TV "White Space"," in *Proc. IEEE ISCCSP*, 2012.
[13] K. Nanavati, "Channel Bonding/Loading for TV White Spaces in IEEE 802.11af," April 2012. http://www.ieee802.org/22/.
[14] S. Shellhammer, S. S. N, R. Tandra, and J. Tomcik, "Performance of Power Detector Sensors of DTV Signals in IEEE 802.22 WRANs," in *Proc. ACM TAPAS*, 2006.
[15] V. Brik, S. Rayanchu, S. Saha, S. Sen, V. Shrivastava, and S. Banerjee, "A Measurement Study of a Commercial-grade Urban WiFi Mesh," in *Proc. ACM IMC*, 2008.
[16] H. Xia, H. Bertoni, L. Maciel, A. Lindsay-Stewart, and R. Rowe, "Microcellular Propagation Characteristics for Personal Communications in Urban and Suburban Environments," *IEEE Trans. Veh. Technol.*, vol. 43, pp. 743–752, August 1994.
[17] A. Goldsmith, *Wireless Communications*. Cambridge, UK: Cambridge University Press, 2005.
[18] E. Sousa and J. Silvester, "Optimum Transmission Ranges in a Direct-Sequence Spread-Spectrum Multihop Packet Radio Network," *J. Sel. Areas Commun.*, vol. 8, pp. 762–771, June 1990.
[19] IEEE P802.11af/D4.0, "Part 11: Wireless LAN Medium Access Control (MAC) and Physical Layer (PHY) specifications; Amendment 5: TV White Spaces Operation," April 2013.